

# Voltammetric Determination of Nitrophenols at a Nickel Dimethylglyoxime Complex – Gold Nanoparticle Modified Glassy Carbon Electrode

F.O.G. Olorundare<sup>1</sup>, D. Nkosi<sup>1,\*</sup> and O.A Arotiba<sup>1,2,\*</sup>

<sup>1</sup> Department of Applied Chemistry, University of Johannesburg, South Africa

<sup>2</sup> Centre for Nanomaterials Science Research, University of Johannesburg, South Africa

\*E-mail: [oarotiba@uj.ac.za](mailto:oarotiba@uj.ac.za), [dnkosi@uj.ac.za](mailto:dnkosi@uj.ac.za)

Received: 17 May 2016 / Accepted: 11 July 2016 / Published: 7 August 2016

---

The electrochemical behaviour and detection of *o*-nitrophenol (*o*-NP) and *p*-nitrophenol (*p*-NP) has been studied on a gold nanoparticle - nickel dimethylglyoxime complex (NiDMG) modified glassy carbon electrode (GCE). The electrode was prepared by drop coating nickel dimethylglyoxime complex on a GCE followed by the electrodeposition of gold nanoparticle. Each step in the electrode modification was characterised by cyclic voltammetry (CV), electrochemical impedance spectroscopy (EIS), scanning electron microscopy (SEM) and high resolution scanning electron microscopy (HRSEM). The results showed that nickel dimethylglyoxime complex /gold nanoparticles electrode had improved conductivity, reversibility, and electron transfer rate in selected redox probe than the unmodified GCE. The GCE/NiDMG-AuNP electrode was used in the determination of *o*-NP and *p*-NP in water. Under the optimal conditions, detection limits of 0.58  $\mu\text{M}$  and 0.103  $\mu\text{M}$  were calculated for *o*-NP and *p*-NP respectively. The GCE/NiDMG-AuNP electrode was applied to real sample and the effect of interferences were studied.

---

**Keywords:** nitrophenol; gold nanoparticles, nickel dimethylglyoxime, square wave voltammetry.

## 1. INTRODUCTION

Nitrophenol (NP) is one the eleven common phenolic compounds that are on the United States environmental protection agency priority pollutants list [1]. A legal tolerance level of 0.1  $\mu\text{g L}^{-1}$  has been set for these compounds [2]. These phenolic compounds are widely distributed in the environment due to their extensive use as intermediates in the manufacturing of pharmaceuticals, insecticides, pesticides dyes, plastics, pigments and explosives [3, 4]. A large number of chloro- and nitrophenols compounds are toxic and carcinogenic [4-6]. Furthermore, chronic toxicological effects such as vomiting, difficulty in swallowing, anorexia, liver and kidney damage, headache, fainting and

mental disturbances have been reported in humans as a result of exposures to phenols [4, 6]. Thus the analysis of phenols in environmental samples is important and in this light, numerous methods for the analysis of NPs in environmental samples have been reported.

These methods are mainly spectrophotometric [7] and to a large extent, chromatographic separation. NP isomers are usually determined by gas chromatography combined with other techniques such as mass spectrometry, flame ionization, electron capture, or nitrogen-sensitive detection [8-10]. High performance liquid chromatography [11], capillary zone electrophoresis [12] and UV-vis fluorescence spectroscopies [13] have also been used in the analysis of NPs. These methods have high sensitivity and excellent selectivity but suffer from some drawbacks such as cost, analysis complexity and limitation to laboratory. Electrochemical methods have been used for the quantification of phenols. Moreover, electrochemical approach to phenol detection is motivated by some advantages over the classical methods earlier mentioned. For example, electrochemical techniques are cheaper, simpler to use and portable [2].

Electroanalysis in general is dependent on the chemical performance of the electrode towards the analyte in question. Thus the modification of electrode or chemically modified electrodes (CME) are employed to improve signal. CME can enhance the determination, sensitivity, improve the anti-interference, or decrease the limit of detection. Various materials such as nanoparticles [14-21], dendrimer [22-24] and polymers [25-27] have been used in electrode modification. Some of these materials have been used in the detection of phenols. A  $\beta$ -cyclodextrin functionalised graphene nano sheets has been used to modify glassy carbon electrode (CD-GNs/GCE) for phenol detection [28]. The result obtained indicated that CD-GNs showed good electrochemical behaviour for the redox of *o*-NP which is attributed to the combination of the excellent properties of graphene and cyclodextrin. Also, the electrochemical determination of *o*-NP by square wave voltammetry (SWV) using a nanocomposite poly(propyleneimine) dendrimer and gold nanoparticles modified glassy carbon electrode and exfoliated graphite electrode (PPI-AuNP/GCE and PPI-AuNP/EG) have been reported [23, 29]. The nanocomposite platform enhanced the electrochemical reduction of *o*-NP, hence its detection with good reproducibility. Graphene-chitosan GR-CS nanocomposite film modified electrode was prepared to study the electrochemical behaviour of NPs. The GR-CS/GCE exhibited enhanced electrocatalytic activity toward the two NP isomers, attributed to high electrical conductivity and electrocatalytic activity of graphene [30].

Nickel and nickel compounds have attracted interest in the electrocatalysis of small organic molecules [31]. The catalytic activity of the nickel-dimethylglyoxime complex towards the electrooxidation of methanol/ethanol has been reported using NiDMG modified GCE by successive drop deposition of Ni salt and DMG solutions, followed by the cycling of the working electrode potential in alkaline solution. The result showed that the

NiDMG-based catalyst in a basic aqueous medium could catalyze methanol and ethanol oxidation through an overall four-electron process to produce formate anion (methanol oxidation) and acetate anion (ethanol oxidation) [31]. Another metallic nanoparticle commonly used in CME is gold nanoparticle [26]. AuNPs have distinctive optical and electronic/electrochemical properties, and can be easily functionalised with other chemical moieties with affinity for gold (e.g. thiols) [32, 33]. AuNPs have also been used in electrochemical sensors for phenol detection [34].

The work reports the use a nanocomposite of gold nanoparticle and nickel dimethylglyoxime NiDMG complex as electrode modifier for the determination of *ortho*- and *para*-NP concentration in water.

## 2. EXPERIMENTAL

### 2.1 Materials and reagents

Dimethylglyoxime (DMG) ( $\text{CH}_3\text{C}(\text{=NOH})\text{C}(\text{=NOH})\text{CH}_3$ ), Nickel (II) acetate, ethanol, ammonia solution 25%, *o*-nitrophenol, *p*-nitrophenol were obtained from (Sigma Aldrich, St Louis, MO, USA), while  $\text{KH}_2\text{PO}_4$ ,  $\text{K}_2\text{HPO}_4$ ,  $\text{H}_2\text{SO}_4$ ,  $\text{K}_3\text{Fe}(\text{CN})_6$ ,  $\text{K}_4\text{Fe}(\text{CN})_6$ ,  $\text{HCl}$ , Dimethyl sulfoxide (DMSO), *N,N*-dimethylformamide (DMF) and sodium hydroxide NaOH were purchased from (Merck Chemicals Darmstadt, Germany). A 10 mM stock solution of NPs was prepared in ethanol and made to mark with 0.1 M phosphate buffer saline solution (PBS) pH 7 which was later stored at 4 °C until use. Phosphate buffer saline solution was used as the supporting electrolyte for all electrochemical experiments. All electrochemical measurements were done on a Dropsens  $\mu\text{Stat}$  8000 (Asturias, Spain) and Compactstat electrochemical workstation (Ivium, Netherlands) with the working electrode, counter electrode and reference electrode using a three-electrode configuration.

Working electrode (WE), counter electrode and reference electrode were 3 mm glassy carbon electrode (GCE), platinum wire and Ag/AgCl (3 MCl<sup>-</sup>) electrode respectively. The WE was pre-treated by mechanical polishing according to the following procedure; it was subjected to sequential polishing on a polishing cloth covered with alumina powder of various particle size 1, 0.3 and 0.05  $\mu\text{m}$  respectively. To remove any adherent  $\text{Al}_2\text{O}_3$  particles the electrode surface was rinsed thoroughly with double distilled deionised water and cleaned in an ultrasonic bath containing deionised water for 10 min and ethanol for another 10 min.

All solutions were de-aerated by purging with argon gas for 5 min and maintaining an argon inert atmosphere throughout the experiments.

All aqueous solutions were prepared with Ultra-pure water of resistivity 18.2 MX cm, which was obtained from a Milli-Q Water System (Millipore Corp., Bedford, MA, USA).

### 2.2 Synthesis of Nickel dimethylglyoxime complex

NiDMG was prepared according to Cardoso et al with a little modification [31]. Briefly, 50 mL of 0.02 mol L<sup>-1</sup> DMG in an alcoholic solution were mixed with 50 mL of Ni (II) acetate aqueous solution, immediately followed by the addition of 5 mL of 1.0 mol L<sup>-1</sup> NaOH aqueous solution. The addition of OH<sup>-</sup> anions was to facilitate the formation of NiDMG, a rose-red precipitate. The NiDMG complex was filtered, washed thoroughly with deionised water and then dried at room temperature. The product obtained was characterised with Fourier transform infrared spectroscopy (FTIR) using Perkin Elmer Spectrum100 FTIR spectrometer UK with pure KBR as background. Scanning Electron Microscopy (SEM) images were collected with a SEM-LEICA S 440 instrument and high resolution scanning electron microscopy HRSEM FEI NOVA Nano SEM 2000 couple with EDX, which allows

to determine chemical composition by Energy Dispersive Spectroscopy (EDS). All the samples were previously coated with carbon coating prior to analysis.

### 2.3 Preparation of the modified electrode

#### 2.3.1 NiDMG modification

Prior to each experiment, the GCE surface was polished with polishing cloth covered with alumina powder with various sizes 1, 0.3 and 0.05  $\mu\text{m}$  particle size and sonicated with double deionised water and ethanol until a mirror-like surface was obtained. This was immediately followed with an aliquot of 5  $\mu\text{L}$  NiDMG in DMF/DMSO solution which was added to the pre-treated electrode surface and allowed to dry in air at room temperature. The electrode was then activated in a 0.1 M NaOH solution by successive sweeping between 0 and 0.8 V (versus Ag/AgCl), at a scan rate of 0.1 V  $\text{s}^{-1}$  for 80 cycles before use. The electrode was labelled GCE/NiDMG.

#### 2.3.2 AuNP modification

A glassy carbon electrode (GCE) and the GCE/NiDMG was modified with gold nanoparticles according to the procedure reported by Arotiba et al [35]. Briefly, 10 mM  $\text{HAuCl}_4$  at pH 7 PBS was prepared and cyclic voltammetry (CV) was performed between potentials -0.4 V to 1.1 V for 10 cycles to deposit gold nanoparticles onto the GCE/NiDMG. The modified electrode was rinsed with distilled water and then PBS. It will be referred to as GCE/NiDMG-AuNP and GCE/AuNP (when the AuNP was electrodeposited directly). The GCE/NiDMG-AuNP was electrochemically characterised using CV, SWV and EIS in PBS and  $[\text{Fe}(\text{CN})_6]^{3-/4-}$  electrolytes.

#### 2.3.3 Electron Microscopy

In order to study the morphology of the modifiers on carbon electrode, screen printed carbon electrode was used in place of GCE for ease of mounting onto the sample stub in the microscope. Some samples were sputtered with carbon where necessary to improve image. The samples were then transferred to the SEM/HRSEM specimen chamber and observed at an accelerating voltage of 20 kV, spot size of 8, aperture of 4, and working distance of 15 mm.

## 3. RESULTS AND DISCUSSION

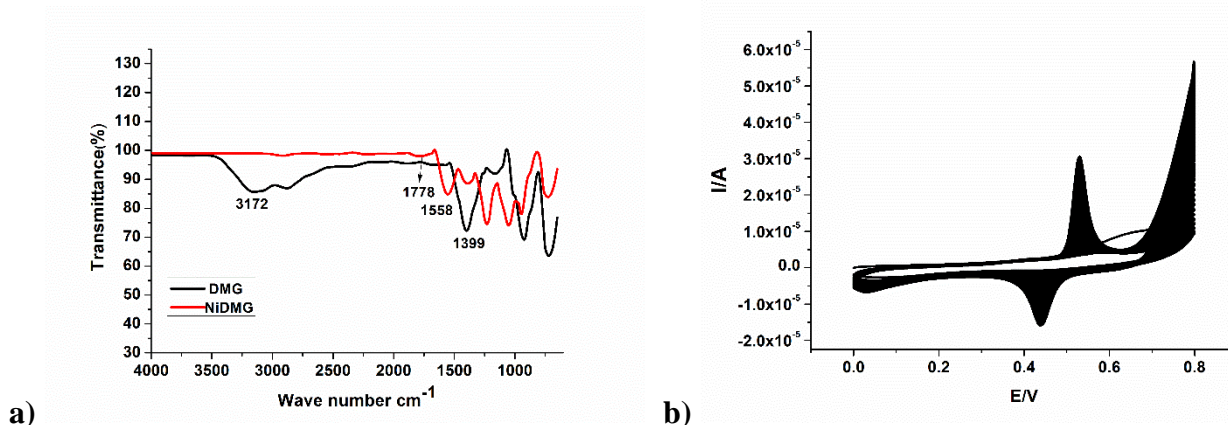
### 3.1 Characterisation of the DMG

Figure 1a shows the FTIR spectra of DMG molecule and NiDMG complex. The broad marked reduction of the broad band  $3172\text{ cm}^{-1}$  suggests that the N-O-H bond stretching mode has become very weak after coordination with Ni(II) i.e the formation of the Ni-N bond in the complex. A new weak band at  $1778\text{ cm}^{-1}$  indicates a strong intramolecular hydrogen bonding in the NiDMG complex. In the spectrum of NiDMG, the band shifted to a high frequency of  $1558\text{ cm}^{-1}$  due to higher C=N bond length [31]. The absorption band at  $1442\text{ cm}^{-1}$  can be assigned to the C=N stretching mode. Furthermore, the

adsorption band at  $1399\text{ cm}^{-1}$  and  $1234\text{ cm}^{-1}$  are attributed to the N–OH bending vibrational and N–O stretching  $1100\text{ cm}^{-1}$  due to the N–O asymmetrical stretching vibration and symmetrical stretching vibration, respectively [36].

### 3.2 Electrochemical characterisation of the NiDMG modified GCE

The cyclic voltammetric interrogation of the NiDMG modified GCE in 1 M NaOH resulted in the formation and progressive increase of the anodic and cathodic peaks between 0.43 and 0.52 V (Fig. 1b) These peaks are due to  $\text{Ni}^{3+}/\text{Ni}^{2+}$  redox process [37, 38]. The shape of the final cyclic voltammogram is very similar to those obtained with electrode formed from nickel macrocyclic-based films in alkaline aqueous solution, which are also similar to those of  $\text{Ni}(\text{OH})_2$  on electrodes [37, 38]. The formation of the peaks can be explained by the formation of the O–Ni–O oxo bridges in alkaline aqueous solution and are indication of the transformation into the ‘O–Ni–O oxo’ bridged forms [37]



**Figure 1.** (a) FTIR spectra of dimethylglyoxime and nickel dimethylglyoxime NiDMG complex. (b) CVs of NiDMG modified GCE in 0.1 M NaOH solution. Scan rate:  $0.1\text{ V s}^{-1}$  (80 cycles).

### 3.3 Scanning Electron Microscopy SEM Characterisation

Figure 2 displays the morphology of the modified electrodes. A dense tubular network of the nickel dimethylglyoxime complex can be observed after drop coating on the carbon electrode (Fig. 2a), while the presence of nanoparticles of gold can be seen after electrodeposition on bare carbon electrode (Fig 2 b a&c). The micrograph on Fig 2c was taken from a high resolution SEM so as to show that the nanoparticles were indeed in the nano size regime. AuNP was electrodeposited on carbon electrode that has been pre-modified with nickel dimethylglyoxime complex i.e. SPCE/NiDMG. The presence of the tubular networks of NiDMG and gold nanoparticles are observed signifying a successful electrodeposition on the SPCE/NiDMG electrode to form SPCE/NiDMG – AuNP. The presence of these two modifiers was confirmed by EDS (Fig. 2e) where peaks due to Ni and Au are seen.

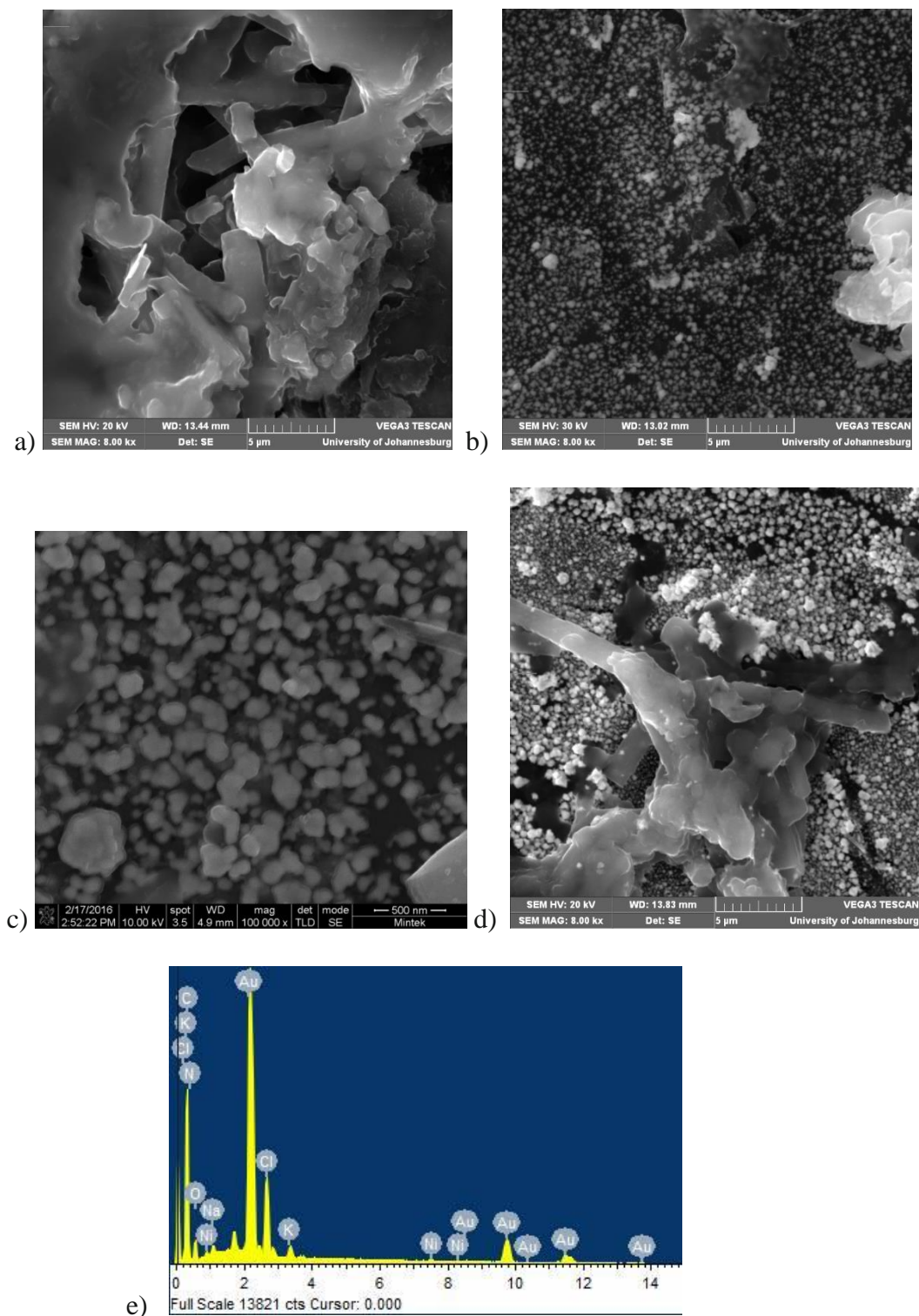


**Figure 2.** SEM images of (a) SPCE/NiDMG, (b) SPCE/AuNP (c) SPCE/AuNP (HR SEM) (d) SPCE/NiDMG – AuNP (e) EDS of SPCE/ NiDMG – AuNP

### 3.4 Electrochemical characterisation of the modified electrode

The electrochemical behaviours of the modified electrodes were investigated to determine their suitability for electroanalysis using  $[\text{Fe}(\text{CN})_6]^{3-/4-}$  as redox probe. As expected, GCE/NiDMG gave the

lowest peak currents and also the most sluggish kinetics (from the large  $\Delta E$ ) as shown in Fig. 3a. This can be attributed to the organic nature of the DMG ligand which deterred electron transfer at the GCE/[Fe(CN)<sub>6</sub>]<sup>3-/4-</sup> interface. Both GCE/NiDMG-AuNP and GCE/AuNP electrodes gave higher peak currents and faster electron transfer kinetics when compared the bare GCE. This observation is in favour of the application of the NiDMG-AuNP as a suitable modifier. It was interesting to note that the electrodeposition of AuNP on the GCE/NiDMG electrode resulted in peak current enhancement in comparison to bare GCE. We believe that the presence of the complex must have assisted in the electrodeposition by providing a larger surface area and distribution of the AuNP.

The enhancing effect of the GCE/NiDMG during the electrodeposition of gold is supported by the electrochemical impedance spectroscopic (EIS) data in Fig. 3b. The diameter of the semicircle in the Nyquist (called the charge transfer resistance, R<sub>ct</sub>) can be used as an indication of electron transfer at the electrode interface. The larger the semicircle the slower the rate of electron transfer. The R<sub>ct</sub> values of both GCE/NiDMG and GCE/NiDMG-AuNP are lower than that of bare GCE in agreement with the CV. However electrode with the fastest electron transfer kinetics is GCE/NiDMG-AuNP denoting its potential for electrochemical analysis.

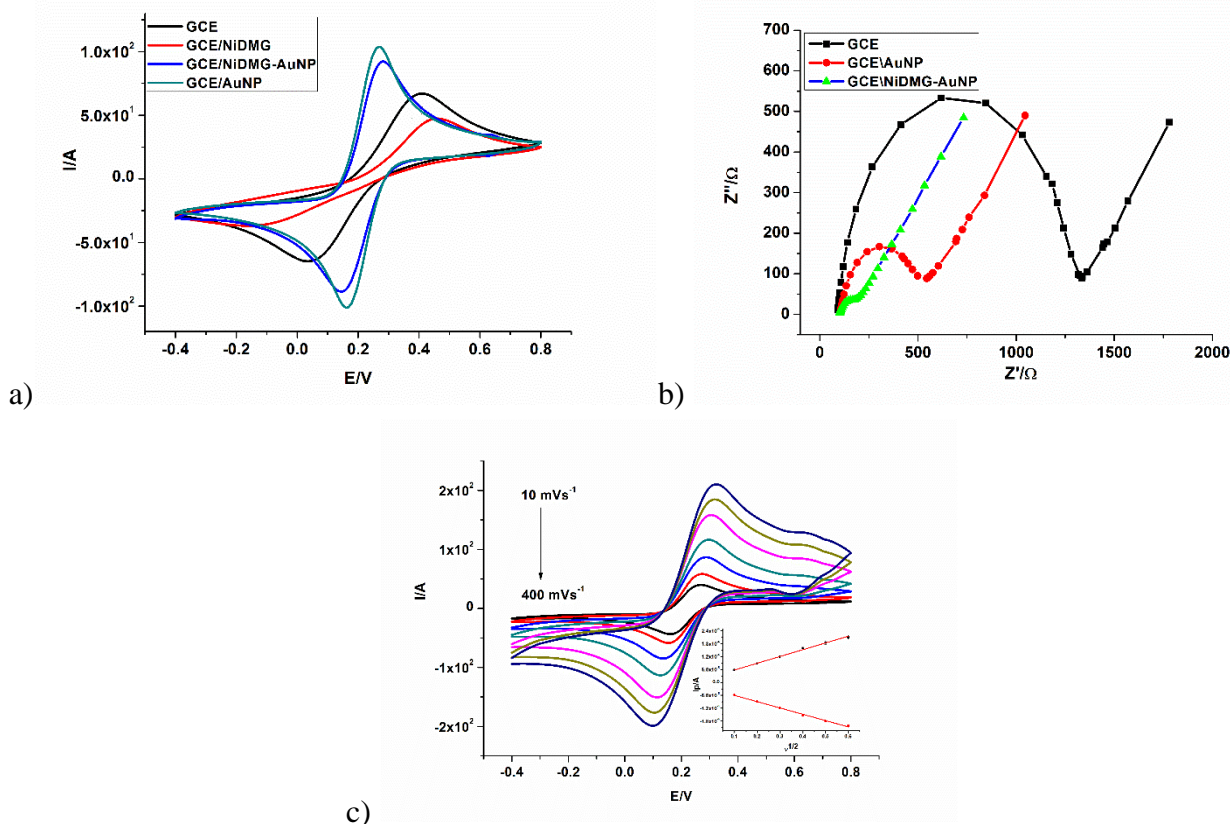


**Figure 3.** (a): CVs of the electrodes in 5 mM [Fe(CN)<sub>6</sub>]<sup>3-/4-</sup>. (b) EIS of the electrodes in 5 mM [Fe(CN)<sub>6</sub>]<sup>3-/4-</sup> (0.1 to 10<sup>5</sup> Hz at bias potential of 0.220 V). (c) CV at different scan rates GCE/NiDMG-AuNP in 5 mM [Fe(CN)<sub>6</sub>]<sup>3-/4-</sup>.

For electroanalysis, the stability of an electrode modifier is imperative. The stability of the GCE/NiDMG-AuNP was interrogated with CV at different scan rates between  $10 \text{ mVs}^{-1}$  and  $400 \text{ mVs}^{-1}$  in the presence of  $[\text{Fe}(\text{CN})_6]^{3-/4-}$  redox probe (Fig. 3c). There was no marked shift in the cathodic and anodic peak potential as scan rate changes therefore the stability of the NiDMG-AuNP on the GCE can be inferred. Furthermore, the anodic and cathodic peaks currents increased linearly with the square root of the scan rate with a correlation coefficient of 0.9964. This result signifies a diffusion controlled process from the Randles - Sevcik equation in which diffusion coefficient can be calculated. For the modified electrode to be used as a sensor, it is expected that the kinetics of the analyte be a diffusion controlled process.

### 3.5 Electrochemical detection of *o*-NP

Fig.4a reports the CV observed for 5 mM *o*-NP on GCE/NiDMG-AuNP in  $0.1 \text{ mol L}^{-1}$  phosphate buffer at scan rate of  $50 \text{ mVs}^{-1}$ . The blank buffer solution did not show any obvious faradaic current and thus the peak observed in the presence of *o*-NP can be solely attributed to the *o*-NP analyte. A typical cyclic voltammetry of *o*-NP similar to that reported by Ndlovu et al [29] was observed in Fig. 4a. The reactions occurring at each peak and the mechanism has been reported in the literature [29, 39, 40].

Fig. 4b compares the SWV responses of the modified electrodes in the presence of *o*-NP. The electrochemical reduction current of *o*-NP on GCE/NiDMG-AuNP is about 77 % higher than the bare GCE. This marked current increase demonstrate a synergic effect of both NiDMG and AuNP towards the phenol reduction. These two modified provided a larger surface area for the phenol accumulation prior to reduction. The presence of  $\pi$ - $\pi$  interaction between *o*-NP and the DMG may also contribute to the peak enhancement. The possibility of a catalytic effect cannot be ruled out though the peak reduction potential for GCE/NiDMG-AuNP occurs at a slightly lower potential than that of GCE. The GCE/NiDMG-AuNP was therefore used for the detection of *o*-NP owing to its better sensitivity [30, 41].

The effect of pH on the electrochemical reduction of *o*-NP was studied. The optimum pH range was between 4 and 7 [39, 40, 42]. An optimum pH of 7 was chosen and used for the detection of *o*-NP in this study.

The GCE/NiDMG-AuNP was used in the detection standard solutions of *o*-NP (Fig 4d). The experiments were carried out in triplicates and calibration curve is presented as inset in Fig 4d. A linear range between  $19.5 \times 10^{-6} \text{ mol L}^{-1}$  and  $1.25 \times 10^{-3} \text{ mol L}^{-1}$  *o*-NP with a correlation of 0.9910 was calculated. The detection limit was calculated using the formula  $3 \sigma/\text{slope}$ . Where  $\sigma$  is the standard deviation of the blank which was taken from five repeats. The detection limit was found to be  $0.58 \mu\text{M}$ . This is comparable to other values obtained from other electrodes which also have detection limits in the micrometre scale [29, 39, 42].

The stability and reproducibility of the modified electrode were investigated by measuring the response in  $2.5 \times 10^{-4} \text{ M}$  *o*-NP for three days. The electrode was stored at  $4^\circ\text{C}$ . The response of the NiDMG-AuNP modified GCE is  $2.5 \times 10^{-4} \text{ M}$ , *o*-NP provided a relative standard deviation of 6.4%,

demonstrating good reproducibility. The reduction peak current of *o*-NP decreased to 98.2 % after 14 days and to 80 % after thirty days of storage.

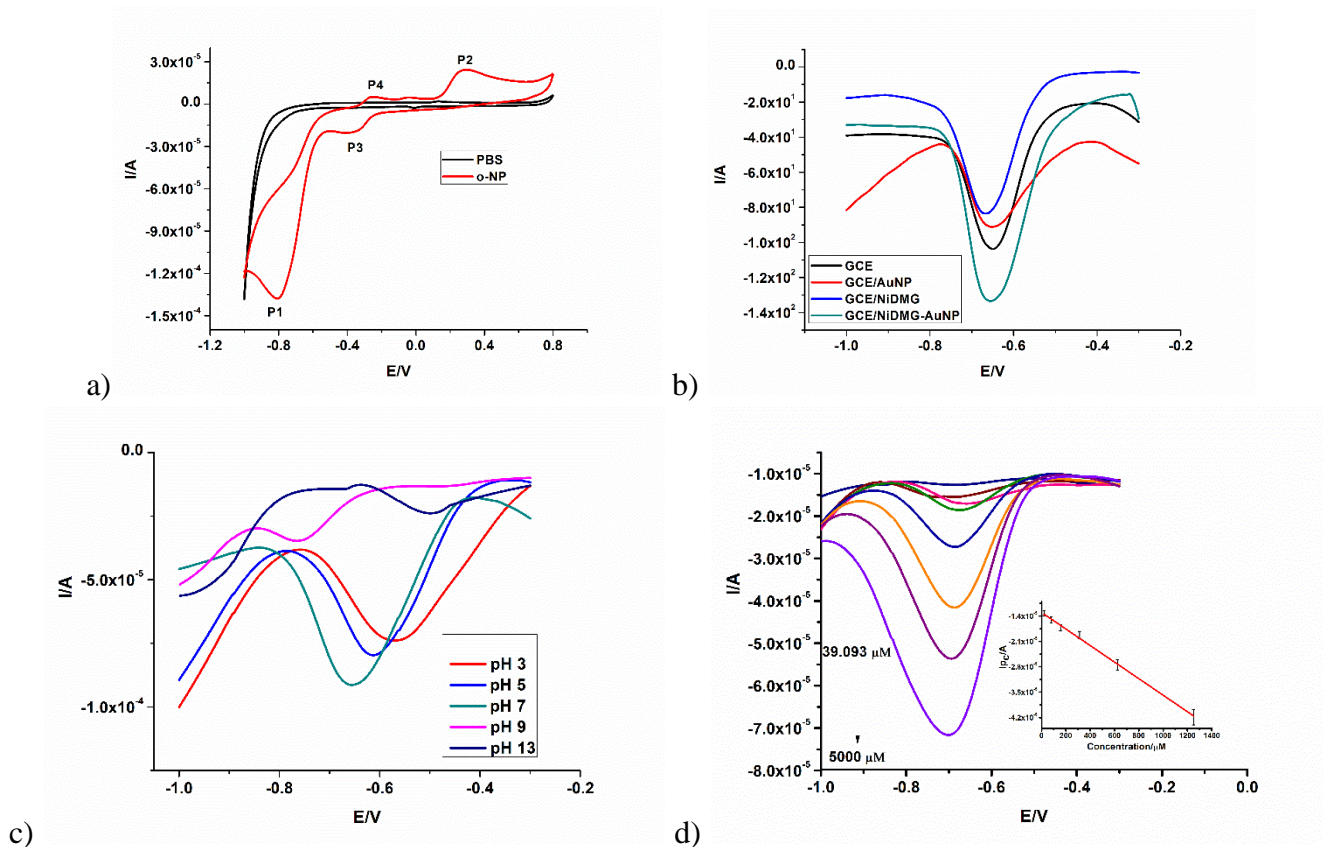


**Figure 4.** (a) CV of 5 mM *o*-NP on GCE/NiDMG-AuNP in 0.1 M PBS at scan rate of 50 mV s<sup>-1</sup>. (b) SWV of 5 mM *o*-NP on the different electrodes in 0.1 M PBS. (c) Effect of pH on GCE/NiDMG-AuNP electrode in a 5 mM solution of *o*-NP. (d) SWV for different concentration of *o*-NP on GCE/NiDMG-AuNP in 0.1 M PBS and Insert Calibration plot showing errors bars.

### 3.6 Electrochemical detection of *p*-NP

A sensor based on the GCE/NiDMG-AuNP platform was also developed for *p*-NP. From Fig. 5a three peaks were observed from the CV of *p*-NP. The electrochemical response of *p*-NP proceeds through two-step reaction mechanism an irreversible reduction peak appears on the cathodic sweep at (P1, E<sub>pc1</sub> = -0.6V) and a pair of reversible peaks (P2, E<sub>pa1</sub> = 0.1V and P3, E<sub>pc2</sub> = 0.0V). In the first step, irreversible reduction of *p*-NP to para-hydroxynitrophenol takes place with the gain of four electrons (4e<sup>-</sup>). The second step involves reversible redox reaction which occurs by the exchange of two electrons, from hydroxynitrophenol to nitrosophenol and vice versa.

The irreversible reduction peak P1 is responsible for the formation of anodic peak P2 and the second cathodic peak P3. The results described in Fig. 5a are consistent with previous works reported

on the detection of *p*-NP [40, 43, 44]. GCE/NiDMG also gave the highest reduction current in the presence of *p*-NP (not shown).

The GCE/NiDMG-AuNP was employed for the determination of *p*-NP using SWV. A linear relationship between the reduction peak current and *p*-NP concentration was obtained from  $5 \times 10^{-7}$  M to  $5 \times 10^{-3}$  M with a linear regression equation of  $y = -2.139768 \times 10^{-8} C (\text{mol L}^{-1}) \times -7.725 \times 10^{-6}$  with a correlation coefficient ( $r^2$ ) of 0.9915 and the limit of detection LOD (S/N = 3) of 0.103  $\mu\text{M}$ .

The detection limits obtained for both *o*-NP and *p*-NP were compared with other reports and presented in Table 1. The comparison of other investigation with the present study showed a very good agreement.

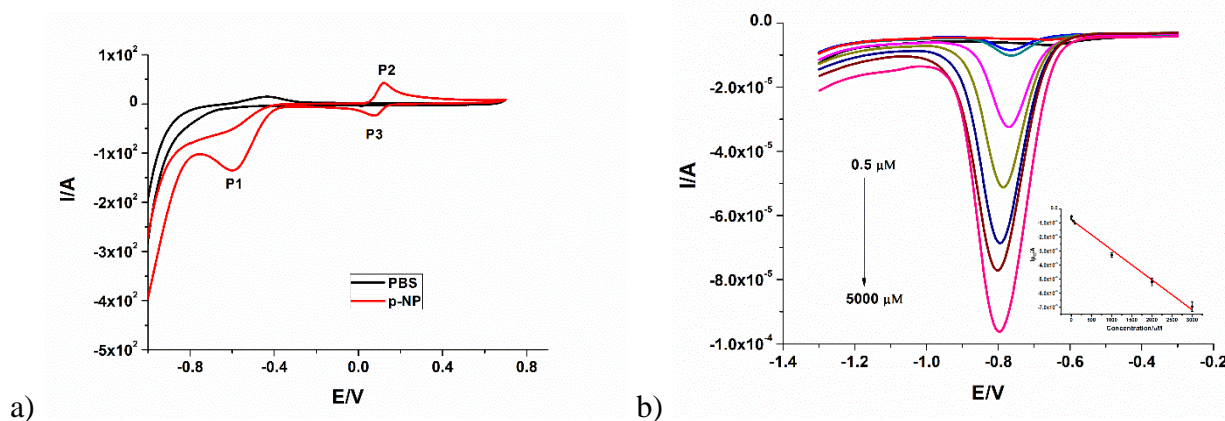


**Figure 5.** (a) Cyclic voltammogram of 3 mM *p*-NP on GCE/NiDMG -AuNP in 0.1 M PBS at scan rate of  $50 \text{ mV s}^{-1}$ . (b) SWV for different concentration of *p*-NP on GCE/NiDMG -AuNP in 0.1 M PBS and insert Calibration plot showing errors bars.

**Table 1.** Comparison of the performances of different electrochemical sensors for *o*-NP and *p*-NP

Modified Electrodes	Method of detection	Linear range ( $\mu\text{M}$ )	Detection limit/Analytes ( $\mu\text{M}$ )	References
HMS/CPE	DPV	0.1 – 40	0.0667 <i>o</i> -NP	[45]
PPI-AuNP /GCE	SWV	0.61 – 625	0.45 <i>o</i> -NP	[29]
Nano-Au /GCE	LSV	10 – 1000	8.0 <i>o</i> -NP	[46]
GO/GCE	LSV	10 – 1000	8.0 <i>p</i> -NP	[47]
$\beta$ -CD-CNS/GCE	DPV	5 – 400	0.3 <i>o</i> -NP	[28]
RGO-AuNP/GCE	DPV,SWV	0.05 – 2.00	0.01, 0.02 <i>p</i> -NP	[34]
OMCs/GCE	DPV	0.5 – 90	0.1 <i>p</i> -NP	[48]
PPI-AuNP/EG	SWV	0.5 – 90	0.08 <i>o</i> -NP	[23]
		0.3 – 50	0.033 <i>o</i> -NP	[23]

GR-CS/GCE	LSV	1 – 240	0.1 <i>o</i> -NP	[30]
		0.1 – 140	0.09 <i>p</i> -NP	
LR-Au LRA/AuE	DPV	0.025 – 1 and 1 – 300	0.02 M <i>p</i> -NP	[49]
MnO <sub>2</sub> -NPs RGO/GCE	LSV	0.02 – 0.5 2 – 180	0.01 <i>p</i> -NP	[44]
NPPy/SDS /GCE	SWV	0.0001 – 100	0.0001 <i>p</i> -NP	[50]
ZnO - Fe <sub>2</sub> O <sub>3</sub> NP/Au	Amperomet ry	10 – 100 1– 10	3.52 0.832 <i>p</i> -NP	[43]
ZnO NPs/Au SWCNT/GCE	DPV	0 – 2.0	0.0077 <i>p</i> -NP	[51]
GNS-FePc/GCE	CV	100 – 700	10 <i>p</i> -NP	[52]
UNFE/GCE	CV	0.5 – 3000	0.23 <i>p</i> -NP	[16]
5-SSADPAN Nr/GCE	DPV	6.7 – 112.1	3.2 <i>p</i> -NP	[53]
OGSF/GCE	SWV	0.2 – 5.2	0.0375 <i>p</i> -NP	[41]
m-HA p- ECG/GCE	DPV	0.2 – 994	0.27 <i>p</i> -NP	[54]
ZG-2/GCE, ZnO/GCE	CV	10 – 1000	13.0 <i>p</i> -NP	[55]
NiDMG- AuNP/GCE	SWV	19.5 – 1250 0.5– 3000	0.58 <i>o</i> -NP 0.103 <i>p</i> -NP	<b>This work</b>

*Key: LSV - Linear sweep voltammetry, MS/CPE - Hexagonal mesoporous silica modified carbon paste electrode, PPI-AuNP /GCE - Poly(polypropyleneimine) gold nanocomposite modified glassy carbon electrode, Nano-Au /GCE - Nano-gold modified glassy carbon electrode, GO/GCE - graphene oxide (GO) film coated glassy carbon electrode, CD-CNS/GCE -  $\beta$  - cyclodextrin functionalised graphene nanosheets modified with glassy carbon electrode, RGO AuNP/GCE - reduced graphene oxide-gold nanoparticle composite modified glassy carbon electrode, OMCs/GCE - ordered mesoporous carbon modified glassy carbon electrode, PPI-AuNP/EG - Poly(polypropyleneimine) gold nanocomposite modified exfoliated graphite electrode, GR-CS/GCE - Graphene-chitosan composite modified glassy carbon electrode, LR-AuLRA/AuE - lamellar ridge-Au Lamellar-ridge architecture gold electrode, MnO<sub>2</sub>-NPs RGO/GCE - Manganese dioxide nanoparticles (MnO<sub>2</sub>-NPs) over reduced graphene oxide (RGO), NPPy/SDS /GCE - nano polypyrrole/sodium dodecyl sulphate film, ZnO - Fe<sub>2</sub>O<sub>3</sub> NP/Au, ZnO NPs/Au – Zinc oxide and hematite (Fe<sub>2</sub>O<sub>3</sub>) nanoparticles (NPs), SWCNT/GCE - Single walled carbon nanotube glassy carbon electrode, GNS-FePc/GCE - graphene nanosheets (GNS) decorated iron phthalocyanine (FePc) film modified electrode, UNFE/GCE - uniform nanoparticle film electrode (UNFE) of glassy carbon (GC), 5-SSADPAN Nr/GCE - 5-sulfosalicylic acid doped polyaniline nanorods modified glassy carbon electrode, OGSF/GCE- organosmectite film-modified glassy carbon electrode, m-HA p-ECG/GCE - Edge –*

carboxylated graphene anchoring magnetite hydroxyl apatite nanocomposite modified glassy carbon electrode, ZG-2/GCE, ZnO/GCE - 3Dimensional flowers shaped zinc glycerolate (ZG-2) and ZnO microstructure modified glassy carbon electrode, NiDMG-AuNP/GCE - Nickel dimethylglyoxime complex gold nanoparticles modified glassy carbon electrode.

### 3.7 Real sample measurement.

The GCE/NiDMG-AuNP was used to detect *o*-NP and *p*-NP in a real water sample – an effluent from an industry. The samples were spiked and the recovery is shown in table 2. The results show that the effect of matrix is not pronounced on the electrochemical sensor thus supporting its analytical suitability.

Sample	Concentration added	Amount found	% Recovery
<i>o</i> -nitrophenol	5.0 $\mu\text{M}$	4.32 $\mu\text{M}$	87
<i>p</i> -nitrophenol	10 $\mu\text{M}$	9.24 $\mu\text{M}$	92

### 3.8 Interference studies and co-detection of *o*-NP and *p*-NP

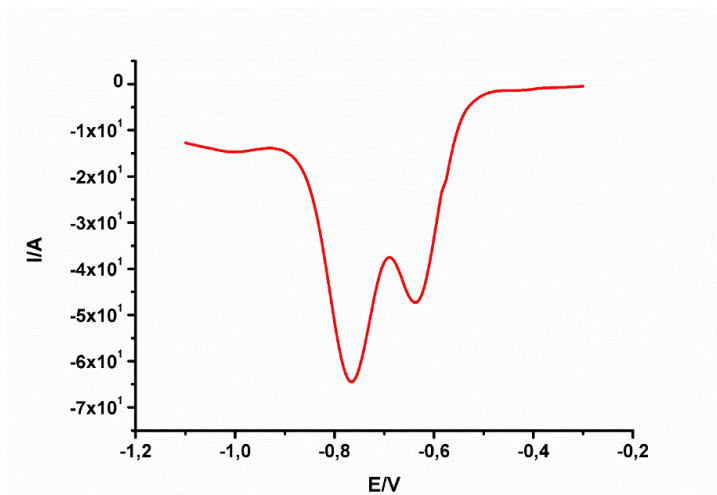


**Figure 6.** SWV showing co-detection of both  $1 \times 10^{-3}$  M *o*-NP and *p*-NP

The influence of, 2-chlorophenol, 3-chlorophenol, 4-chlorophenol and bisphenol A (BPA) on the reduction signal were determined for *o*-NP and *p*-NP. These phenolic compounds showed no interference with the *o*-NP electrochemical signal owing to the fact that they do not have reducible nitro-group and their hydroxyl group reduction occurs out of the working potentials for *o*-NP. The result suggest that the GCE/NiDMG-AuNP may be employed for practical analysis. Furthermore, in the presence of *o*-NP, the GCE/NiDMG-AuNP lost 17% of the initial reduction current (at scan 1) at the fifth scan, in comparison to a loss of 29% current at the bare GCE electrode showing that the GCE/NiDMG-AuNP was more resistant to fouling.

The square wave voltammetric response of a mixture of *o*-NP and *p*-NP was carried out. Fig. 6 shows that the mixture has two different reductive peak current signatures on the GCE/NiDMG-AuNP: -0.78 V for *p*-NP and the -0.6 for *o*-NP. This results suggest this possibility of co-detecting these two phenols in solution.

#### 4. CONCLUSION

A simple method of depositing AuNP on a nickel DMG complex has been described. Though the use of AuNP as a sensor platform is well reported, this work shows the possibility of electrodepositing AuNP on a metal complex and its applicability as a sensor for ortho and para nitrophenol. The synergic effect of NiDMG-AuNP platform reported can be explored in the detection of other analytes.

#### ACKNOWLEDGEMENT

The authors would like to acknowledge the Centre for Nanomaterials Science Research, University of Johannesburg and the National Research Foundation (NRF) South Africa for funding this research project.

#### References

1. USEPA, Persistent Organic Pollutants: A Global issue, A Global Response, in: K. Kovner (Ed.), USEPA United State Environmental Protection Agency Washington DC, 2015.
2. M. Santhiago, C.S. Henry, L.T. Kubota, Low cost, *Electrochimica Acta*, 130 (2014) 771-777.
3. Y. Zeng, Y. Zhou, T. Zhou, G. Shi, *Electrochimica Acta*, 130 (2014) 504-511
4. A. Mehrizad, M. Aghaie, P. Gharbani, S. Dastmalchi, M. Monajjemi, K. Zare, *Iran Journal of Environmental Health Science and Engineering*, (2012). 9
5. S. Chen, Z.P. Xu, Q. Zhang, G.M. Lu, Z.P. Hao, S. Liu, *Separation and Purification Technology*, 67 (2009) 194-200.
6. A.Y. Dursun, O. Tepe, *Journal of hazardous materials*, 126 (2005) 105-111.
7. A. Niazi, A. Yazdanipour, *Journal of hazardous materials*, 146 (2007) 421-427.
8. H. Ghorbanpour, A. Yadeghari, L. Khoshmaram, M.A. Farajzadeh, *Analytical Methods*, 6 (2014) 7733-7743.
9. N.R. Neng, J.M. Nogueira, *Molecules*, 19 (2014) 9369-9379.
10. M. Guidotti, G. Ravaioli, M. Vitali, *Journal of High Resolution Chromatography*, 22 (1999) 628-630.
11. A. Almási, E. Fischer, P. Perjési, *Journal of biochemical and biophysical methods*, 69 (2006) 43-50.
12. X. Guo, Z. Wang, S. Zhou, *Talanta*, 64 (2004) 135-139.
13. C. Nistor, A. Oubiña, M.-P. Marco, D. Barceló, J. Emnéus, *Analytica chimica acta*, 426 (2001) 185-195.
14. T. Kuilla, S. Bhadra, D. Yao, N.H. Kim, S. Bose, J.H. Lee, *Progress in polymer science*, 35 (2010) 1350-1375.
15. R.N. Goyal, S. Bishnoi, *Indian Journal of Chemistry-Part A Inorganic Physical Theoretical and Analytical*, 51 (2012) 205.

16. P. Wang, J. Xiao, A. Liao, P. Li, M. Guo, Y. Xia, Z. Li, X. Jiang, W. Huang, *Electrochimica Acta*, 176 (2015) 448-455.
17. N.D. Dimcheva, E.G. Horozova, *Chemical Papers*, 69 (2015) 17-26.
18. S. Navalon, A. Dhakshinamoorthy, M. Alvaro, H. Garcia, *Coordination Chemistry Reviews*, 312 (2015) 99-148.
19. W.Q. Lim, Z. Gao, *Electroanalysis*, 27 (2015) 2074-2090.
20. K. Lawrence, C.L. Baker, T.D. James, S.D. Bull, R. Lawrence, J.M. Mitchels, M. Opallo, O.A. Arotiba, K.I. Ozoemena, F. Marken, *Chemistry—An Asian Journal*, 9(5) (2014) 1226-1241.
21. A.S. Adekunle, J.G. Ayenimo, X.Y. Fang, W.O. Doherty, O.A. Arotiba, B.B. Mamba, *International Journal of Electrochemical Science*, 6 (2011) 2826-2844.
22. F. Li, J. Peng, Q. Zheng, X. Guo, H. Tang, S. Yao, *Analytical chemistry*, 87(9) (2015) 4806-4813.
23. T. Ndlovu, O.A. Arotiba, B.B. Mamba, *International Journal of Electrochemical Science*, 9 (2014) 8330-8339.
24. T. Ndlovu, O.A. Arotiba, S. Sampath, R.M.W. Krause, and B.B. Mamba, *Journal of Applied Electrochemistry*, 41 (12) (2011) 1389-1396.
25. J S. Jabeen, A. Kausar, B. Muhammad, S. Gul, M. Farooq, *Polymer-Plastics Technology and Engineering*, 54 (2015) 1379-1409.
26. C. Wang, C. Yu, *Reviews in Analytical Chemistry*, 32 (2013) 1-14.
27. J. Wang, D. Zhang, *Advances in Polymer Technology*, 32 (2013) E323-E368.
28. J. Liu, Y. Chen, Y. Guo, F. Yang, F. Cheng, *Journal of Nanomaterials*, 2013 (2013) 11.
29. T. Ndlovu, O.A. Arotiba, R.W. Krause, B.B. Mamba, *International Journal of Electrochemical Science*, 5 (2010) 1179-1186.
30. J. Tang, L. Zhang, G. Han, Y. Liu, W. Tang, *Journal of The Electrochemical Society*, 162 (2015) B269-B274.
31. W.S. Cardoso, V.L. Dias, W.M. Costa, I. de Araujo Rodrigues, E.P. Marques, A.G. Sousa, J. Boaventura, C.W. Bezerra, C. Song, H. Liu, *Journal of Applied Electrochemistry*, 39 (2009) 55-64.
32. D.A. Giljohann, D.S. Seferos, W.L. Daniel, M.D. Massich, P.C. Patel, C.A. Mirkin, *Angewandte Chemie International Edition*, 49 (2010) 3280-3294.
33. K. Saha, S.S. Agasti, C. Kim, X. Li, V.M. Rotello, *Chemical reviews*, 112 (2012) 2739-2779.
34. Y. Tang, R. Huang, C. Liu, S. Yang, Z. Lu, S. Luo, *Analytical Methods*, 5 (2013) 5508-5514.
35. O. Arotiba, J. Owino, E. Songa, N. Hendricks, T. Waryo, N. Jahed, P. Baker, E. Iwuoha, *Sensors*, 8 (2008) 6791-6809.
36. J S. Jadhav, S. Kulkarni, S. Quadri, *Journal of Chemistry and Chemical Sciences*, 5 (2015) 311-316.
37. B. Agboola, T. Nyokong, *Electrochimica acta*, 52 (2007) 5039-5045.
38. M. Ureta-Zanartu, A. Alarcon, C. Berrios, G. Cardenas-Jiron, J. Zagal, C. Gutierrez, *Journal of electroanalytical chemistry*, 580 (2005) 94-104.
39. J. Fischer, L. Vanourkova, A. Danhel, V. Vyskocil, K. Cizek, J. Barek, K. Peckova, B. Yosypchuk, T. Navratil, *International Journal of Electrochemical Science*, 2 (2007) 226-234
40. M. El Mhammedi, M. Achak, M. Bakasse, A. Chtaini, *Journal of Hazardous Materials*, 163 (2009) 323-328.
41. G.B. Ngassa, I.K. Tonlé, E. Ngameni, *Talanta*, 147 (2016) 547-555.
42. L.Q. Luo, X.I. Zou, Y.P. Ding, Q.S. Wu, *Sensors and Actuators B: Chemical*, 135 (2008) 61-65.
43. K. Singh, A. Kaur, A. Umar, G.R. Chaudhary, S. Singh, S.K. Mehta, *Journal of Applied Electrochemistry*, 45 (2015) 253-261.
44. S.A. Zaidi, J.H. Shin, *RSC Advances*, 5 (2015) 88996-89002.
45. C. Zhou, Z. Liu, Y. Dong, D. Li, *Electroanalysis*, 21 (2009) 853-858.
46. L. Chu, L. Han, X. Zhang, *Journal of Applied Electrochemistry*, 41 (2011) 687-694.
47. J. Li, D. Kuang, Y. Feng, F. Zhang, Z. Xu, M. Liu, *Journal of Hazardous Materials*, 201 (2012) 250-259.

48. T. Zhang, Q. Lang, D. Yang, L. Li, L. Zeng, C. Zheng, T. Li, M. Wei, A. Liu, *Electrochimica Acta*, 106 (2013) 127-134.
49. X. Guo, H. Zhou, T. Fan, D. Zhang, , *Sensors and Actuators B: Chemical*, 220 (2015) 33-39.
50. A.D. Arulraj, M. Vijayan, V.S. Vasantha, *Analytica chimica acta*, 899 (2015) 66-74.
51. M. Govindhan, T. Lafleur, B.R. Adhikari, A. Chen, *Electroanalysis*, 27 (2015) 902-909.
52. R. Devasenathipathy, V. Mani, S.-M. Chen, K. Manibalan, S.T. Huang, *International Journal of Electrochemical Science*, 10 (2015) 1384-1392.
53. R. Suresh, K. Giribabu, R. Manigandan, S. Praveen Kumar, S. Munusamy, S. Muthamizh, V. Narayanan, *Analytical Letters*, 49 (2016) 269-281.
54. G. Bharath, V. Veeramani, S.M. Chen, M. Rajesh, M.M. Raja, A. Balamurugan, D. Mangalaraj, C. Viswanathana, N. Ponpandian, *RSC Advances*, 5 (2015) 13392–13401.
55. A. Sinhamahapatra, D. Bhattacharjya, J.S. Yu, *RSC Advances*, 5 (2015 ) 37721–37728.

© 2016 The Authors. Published by ESG ([www.electrochemsci.org](http://www.electrochemsci.org)). This article is an open access article distributed under the terms and conditions of the Creative Commons Attribution license (<http://creativecommons.org/licenses/by/4.0/>).